

X-ray Absorption Pre-Edge Studies of High-Spin Iron(II) Complexes

Clayton R. Randall,[†] Lijin Shu,[†] Yu-Min Chiou,[†] Karl S. Hagen,[‡] Masami Ito,[§]
Nobumasa Kitajima,^{§,||} Rene J. Lachicotte,[‡] Yan Zang,[†] and Lawrence Que, Jr.,^{*,†}

Department of Chemistry, University of Minnesota, Minneapolis, Minnesota 55455, Department of Chemistry, Emory University, Atlanta, Georgia 30322, and Research Laboratory of Resources Utilization, Tokyo Institute of Technology, 4259 Nagatsuta, Midori-ku, Yokohama 227, Japan

Received October 28, 1994[⊗]

Fe K-edge X-ray absorption spectroscopy is utilized to study a series of 22 synthetic high-spin iron(II) complexes. The 1s → 3d pre-edge peak of each complex is quantitated and compared with the others in order to explore its correlation with the coordination number and symmetry of the iron center. Like the high-spin iron(III) complexes (Roe, A. L.; Schneider, D. J.; Mayer, R. J.; Pyrz, J. W.; Que, L., Jr. *J. Am. Chem. Soc.* **1984**, *106*, 1676–1681), the iron(II) complexes can be grouped on the basis of their normalized pre-edge peak intensities: the six-coordinate complexes have pre-edge areas from 4 to 6 units, the five-coordinate from 8 to 13 units, and the tetrahedral 16 to 21 units. Three six-coordinate “iron(II)” nitrosyl complexes examined have pre-edge areas comparable to those of normal iron(II) five-coordinate complexes due to their highly distorted geometry. The information obtained here can be used to determine the coordination number of the high-spin iron(II) centers in iron(II)-containing proteins and other model complexes and to complement analyses based on extended X-ray absorption fine structure (EXAFS).

Introduction

X-ray absorption spectroscopy, in particular EXAFS (extended X-ray absorption fine structure),¹ has been very useful in determining the coordination chemistry of metal centers in a wide variety of materials.² However, EXAFS has an inherent uncertainty of approximately 20% in determining coordination number. X-ray absorption pre-edge and edge features carry useful information that can help to resolve this uncertainty and have the advantages of rapid data collection and little necessary workup. A small pre-edge peak in the spectra of transition metal complexes with incompletely filled d shells has been assigned to the 1s → 3d transition.³ This transition has different intensities for octahedral and tetrahedral complexes and has been used to infer site symmetry in metal complexes.⁴

The pre-edge spectra of iron complexes show features at approximately 7112–7113 eV that can be assigned to the iron 1s → 3d transition.³ A previous study of 28 synthetic iron(III) complexes that included molecular orbital calculations⁵ indicated that the intensity of these pre-edge features relative to the K-edge absorption intensity can be correlated with the amount of iron 4p and 3d orbital mixing and therefore with the coordination

geometry around the iron atom. The pre-edge intensity generally increases with a decrease in coordination number and departure from a centrosymmetric coordination environment, *i.e.* $I_{\text{octahedral}} < I_{\text{5-coord}} < I_{\text{tetrahedral}}$. We have used this compilation of data successfully to determine the probable coordination geometries of the iron centers in several nonheme iron-containing proteins.^{5–8} This collection of data has been applied by other groups to various iron proteins^{9–14} and has served as a precedent for the study of manganese,¹⁵ cobalt,¹⁶ nickel,¹⁷ and copper¹⁸ sites in proteins.

There is, however, a growing list of proteins that have iron(II) centers in their active sites, including deoxyhemerythrin,¹⁹ ribonucleotide reductase,²⁰ the hydroxylase component of

[†] University of Minnesota.

[‡] Emory University.

[§] Tokyo Institute of Technology.

^{||} Deceased January 8, 1995.

[⊗] Abstract published in *Advance ACS Abstracts*, February 1, 1995.

- (1) Abbreviations used: acac, 2,4-pentanedionate(1-); BF, benzoylformate; BPMP, 2,6-bis((bis(2-pyridylmethyl)amino)methyl)-4-methylphenol; cyclen, 1,4,7,10-tetraazacyclododecane; HB(Pr₂pz)₃, hydrotris(3,5-diisopropylpyrazol-1-yl)borate(1-); HPTB, *N,N,N',N'*-tetrakis(2-benzimidazolylmethyl)-2-hydroxy-1,3-diaminopropane; HPTP, *N,N,N',N'*-tetrakis(2-pyridylmethyl)-2-hydroxy-1,3-diaminopropane; py, pyridine; 6TLA, tris((6-methyl-2-pyridyl)methyl)amine; TMPzA, tris(3,5-dimethylpyrazol-1-ylmethyl)amine; TPA, tris(2-pyridylmethyl)amine.
- (2) (a) Cramer, S. P.; Hodgson, K. O. *Prog. Inorg. Chem.* **1979**, *25*, 1–39. (b) Cramer, S. P. In *X-ray Absorption*; Koningsberger, D. C., Prins, R., Eds.; Wiley: New York, 1988; pp 257–320.
- (3) Shulman, R. G.; Yafet, Y.; Eisenberger, P.; Blumberg, W. E. *Proc. Natl. Acad. Sci. U.S.A.* **1976**, *73*, 1384–1388.
- (4) Srivastava, U. C.; Nigam, H. L. *Coord. Chem. Rev.* **1972**, *9*, 275–310.
- (5) Roe, A. L.; Schneider, D. J.; Mayer, R. J.; Pyrz, J. W.; Que, L., Jr. *J. Am. Chem. Soc.* **1984**, *106*, 1676–1681.

- (6) Scarrow, R. C.; Maroney, M. J.; Palmer, S. M.; Que, L., Jr.; Roe, A. L.; Salowe, S. P.; Stubbe, J. *J. Am. Chem. Soc.* **1987**, *109*, 7857–7864.
- (7) True, A. E.; Orville, A. M.; Pearce, L. L.; Lipscomb, J. D.; Que, L., Jr. *Biochemistry* **1990**, *29*, 10847–10854.
- (8) True, A. E.; Scarrow, R. C.; Randall, C. R.; Holz, R. C.; Que, L., Jr. *J. Am. Chem. Soc.* **1993**, *115*, 4246–4255.
- (9) Kauzlarich, S. M.; Teo, B. K.; Zirino, T.; Burman, S.; Davis, J. C.; Averill, B. A. *Inorg. Chem.* **1986**, *25*, 2781–2785.
- (10) Zhang, K.; Stern, E. A.; Ellis, F.; Sanders-Loehr, J.; Shiemke, A. K. *Biochemistry* **1988**, *27*, 7470–7479.
- (11) Tsang, H.-T.; Batie, C. J.; Ballou, D. P.; Penner-Hahn, J. E. *Biochemistry* **1989**, *28*, 7233–7240.
- (12) Yang, C. Y.; Heald, S. M.; Tranquada, J. M.; Xu, Y.; Wang, Y. L.; Moodenbaugh, A. R.; Welch, D. O.; Suenaga, M. *Phys. Rev.* **1989**, *B39*, 6681–6689.
- (13) Kim, S.; Bae, I. T.; Sandifer, M.; Ross, P. N.; Carr, R.; Woicik, J.; Antonio, M. R.; Scherson, D. A. *J. Am. Chem. Soc.* **1991**, *113*, 9063–9066.
- (14) Cartier, C.; Momenteau, M.; Dartyge, E.; Fontaine, A.; Tourillon, G.; Michalowicz, A.; Verdager, M. *J. Chem. Soc., Dalton Trans.* **1992**, 609–618.
- (15) Penner-Hahn, J. E.; Fronko, R. M.; Pecoraro, V. L.; Yocum, C. F.; Betts, S. D.; Bowlby, N. R. *J. Am. Chem. Soc.* **1990**, *112*, 2549–2557.
- (16) Wirt, M. D.; Sagi, I.; Chen, E.; Frisbie, S. M.; Lee, R.; Chance, M. R. *J. Am. Chem. Soc.* **1991**, *113*, 5299–5304.
- (17) Colpas, G. J.; Maroney, M. J.; Bagyinka, C.; Kumar, M.; Willis, W. S.; Suib, S. L.; Baidya, N.; Mascharak, P. K. *Inorg. Chem.* **1991**, *30*, 920–928.
- (18) Sano, M.; Komorita, S.; Yamatera, H. *Inorg. Chem.* **1992**, *31*, 459–463.

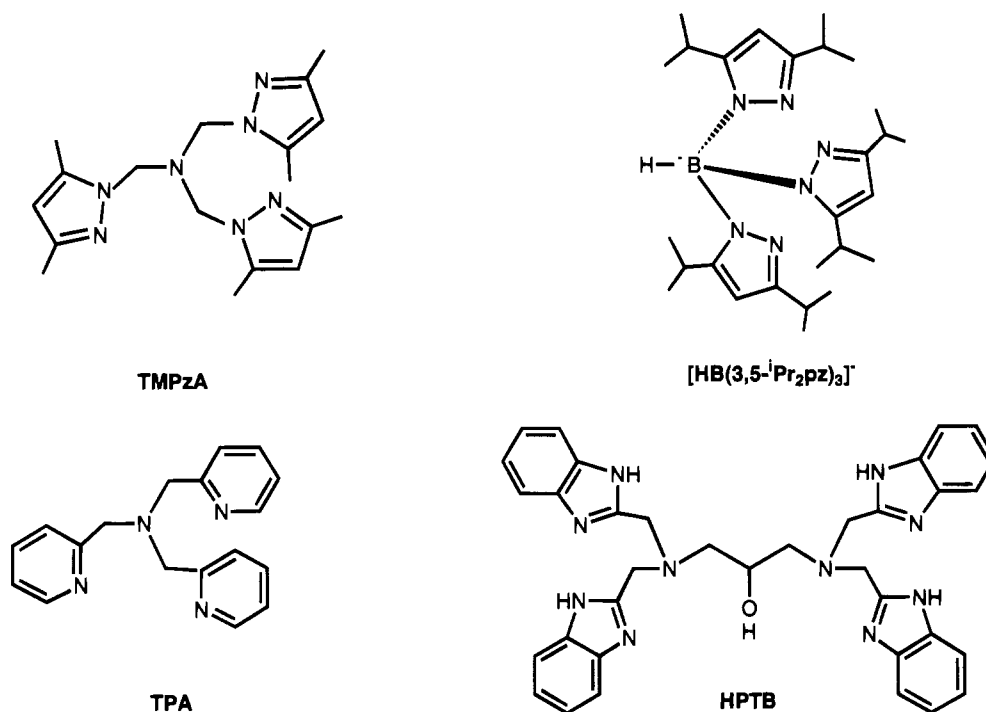


Figure 1. Examples of ligands used to prepare model complexes for this study of $1s \rightarrow 3d$ pre-edge peak areas.

methane monooxygenase,²¹ soybean lipoxygenase,²² isopenicillin N synthase,²³ and extradiol cleaving catechol dioxygenases.²⁴ Many of these enzymes are involved in oxygen transport and metabolism.²⁵ Because the transition probabilities associated with the $1s \rightarrow 3d$ features in iron(III) and iron(II) complexes may differ, the range of values established by the pre-edge data compiled by Roe *et al.*⁵ for iron(III) centers may not exactly apply to the coordination geometries of iron(II) centers. In this paper, that previous work is extended to high-spin iron(II) complexes. We have taken advantage of the increased number of structurally characterized high-spin iron(II) complexes available due to the interest in the enzymes mentioned above and compiled a database for the $1s \rightarrow 3d$ pre-edge features of these complexes that can be used to determine the coordination number and probable geometry of iron(II) centers.

Experimental Procedures

The model complexes used in this study were prepared as described in the reference of Table 1, except for $(\text{NEt}_4)_2[\text{FeCl}_4]$, which was prepared according to a modification of the procedure used by Lauher

and Ibers.²⁶ The material was determined to be authentic on the basis of fitting its EXAFS spectrum according to previously published procedures.⁶ Four Fe-Cl scatterers were found at $2.31 \pm 0.02 \text{ \AA}$, in good agreement with the crystallographically obtained value of 2.29 \AA .²⁶ Some of the ligands used to prepare the model complexes are shown in Figure 1.

X-ray absorption spectra (XAS) were collected between 6.9 and 8.1 keV at station C2 of the Cornell High Energy Synchrotron Source (CHESS) and at beamline X9 of the National Synchrotron Light Source (NSLS) at Brookhaven National Laboratory. The monochromator was calibrated by using the $1s \rightarrow 3d$ feature at 7113.0 eV in the XAS spectrum of $(\text{NEt}_4)[\text{FeCl}_4]$. The XAS data for all iron(II) model complexes except $(\text{NEt}_4)_2[\text{FeCl}_4]$ were obtained in transmission mode ($A_{\text{exp}} = -\log(I/I_0)$) as dispersions of the microcrystalline solids in boron nitride at room temperature. The XAS data for $(\text{NEt}_4)_2[\text{FeCl}_4]$ were obtained in fluorescence mode ($A_{\text{exp}} = C/I_0$) as a boron nitride dispersion at 50 K, using a 13-element Canberra germanium diode array fluorescence detector. The fluorescence data were not corrected for absorption because of the normalization procedure used (*vide infra*).

The pre-edge areas were calculated as previously described⁵ by subtracting an arctangent function from the data and normalizing with respect to the edge jump height. The background function was determined by a least-squares fit of an arctangent together with a first-order polynomial to the data below the inflection point of the edge. The regions fit were typically from -60 to -5 eV with respect to the inflection point, not including the position of the pre-edge peak $\pm \sim 4$ eV. The area of the pre-edge peak after the background subtraction was obtained by integrating over a range of ~ 8 eV. This range centered on the peak and any residual background function were interpolated over that range. The edge jump was determined by fitting first-order polynomials to the data, from -50 to -18 eV and from 150 to 325 eV with respect to the inflection point of the edge. The difference between these two lines at the inflection point was used as the normalization factor for the pre-edge peak area. The normalized pre-edge area is reported as percent of edge height \times eV.⁵ For example, $(\text{NEt}_4)_2[\text{FeCl}_4]$ has a normalized pre-edge area of 0.174 eV, which is abbreviated as 17.4 units.

Results and Discussion

The iron(II) complexes chosen for this study all exhibit features approximately 10 eV less than the inflection point of

- (19) Holmes, M. A.; Trong, I. L.; Turley, S.; Sieker, L. C.; Stenkamp, R. E. *J. Mol. Biol.* **1991**, *218*, 583–593.
- (20) (a) Nordlund, P.; Sjöberg, B.-M.; Eklund, H. *Nature* **1990**, *345*, 593–598. (b) Åberg, A. Ph.D. Thesis, Stockholm University, 1993.
- (21) (a) Fox, B. G.; Surerus, K. K.; Münck, E.; Lipscomb, J. D. *J. Biol. Chem.* **1988**, *263*, 10553–10556. (b) Rosenzweig, A. C.; Frederick, C. A.; Lippard, S. J.; Nordlund, P. *Nature* **1993**, *366*, 537–543.
- (22) (a) Minor, W.; Steczko, J.; Bolin, J. T.; Otwinowski, Z.; Axelrod, B. *Biochemistry* **1993**, *32*, 6320–6323. (b) Boyington, J. C.; Gaffney, B. J.; Amzel, L. M. *Science* **1993**, *260*, 1482–1486.
- (23) (a) Chen, V. J.; Orville, A. M.; Harpel, M. R.; Frolik, C. A.; Surerus, K. K.; Münck, E.; Lipscomb, J. D. *J. Biol. Chem.* **1989**, *264*, 21677–21681. (b) Ming, L.-J.; Que, L., Jr.; Kriauciunas, A.; Frolik, C. A.; Chen, V. J. *Biochemistry* **1991**, *30*, 11653–11659. (c) Randall, C. R.; Zang, Y.; True, A. E.; Que, L., Jr.; Charnock, J. M.; Garner, C. D.; Fujishima, Y.; Schofield, C. J.; Baldwin, J. E. *Biochemistry* **1993**, *32*, 6664–6673.
- (24) (a) Arciero, D. M.; Lipscomb, J. D.; Huynh, B. H.; Kent, T. A.; Münck, E. *J. Biol. Chem.* **1983**, *258*, 14981–14991. (b) Tatsuno, Y.; Saeki, Y.; Nozaki, M.; Otsuka, S.; Maeda, Y. *FEBS Lett.* **1980**, *112*, 83–85.
- (25) Que, L., Jr. In *Bioinorganic Catalysis*; Reedijk, J., Ed.; Marcel Dekker: New York, 1993; pp 347–393.

(26) Lauher, J. W.; Ibers, J. A. *Inorg. Chem.* **1975**, *14*, 348–352.

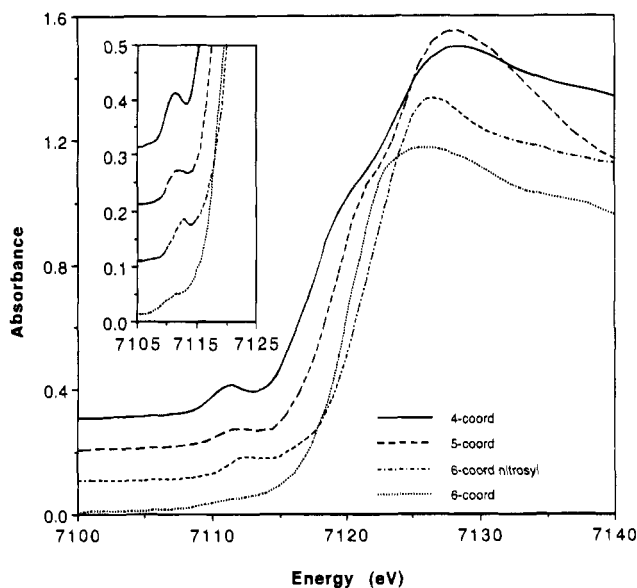


Figure 2. Pre-edge and edge spectra of representative model complexes: —, six-coordinate $[\text{Fe}_2(\text{O}_2\text{CPh})_4(\text{pyridine})_4]$; - - -, six-coordinate $[(\text{TMPzA})\text{Fe}(\text{NO})(\text{Cl})](\text{BPh}_4)$; - · -, five-coordinate $[(\text{HB}(3,5\text{-}^i\text{Pr}_2\text{pz})_3)\text{Fe}(\text{O}_2\text{CPh})]$; · · ·, four-coordinate $[(\text{HB}(3,5\text{-}^i\text{Pr}_2\text{pz})_3)\text{Fe}(\text{SC}_6\text{H}_4\text{-}p\text{-NO}_2)]$.

the K-edge absorption, which are assigned to the $1s \rightarrow 3d$ transition.³ The amplitude of this feature is dependent upon coordination number, as can be seen in Figure 2. The six-coordinate complex shown, $[\text{Fe}_2(\text{O}_2\text{CPh})_4(\text{pyridine})_4]$, has the smallest pre-edge amplitude. In some six-coordinate complexes, the pre-edge feature is little more than a shoulder on the absorption edge (*vide infra*). The six-coordinate nitrosyl complex $[(\text{TMPzA})\text{Fe}(\text{NO})(\text{Cl})](\text{BPh}_4)$, however, has a significantly more intense pre-edge peak, as does the five-coordinate complex $[(\text{HB}(3,5\text{-}^i\text{Pr}_2\text{pz})_3)\text{Fe}(\text{O}_2\text{CPh})]$, with the pre-edge features more clearly resolved from the absorption edge. The distorted tetrahedral complex $[(\text{HB}(3,5\text{-}^i\text{Pr}_2\text{pz})_3)\text{Fe}(\text{SC}_6\text{H}_4\text{-}p\text{-NO}_2)]$ has the largest amplitude, with the pre-edge peak standing out clearly from the absorption edge.

The pre-edge peak areas of the iron(II) complexes chosen for this study are given in Table 1. Half (11 out of 22) of the complexes chosen have carboxylate ligands, in part because carboxylate ligation is a recurring feature in a number of proteins with iron(II) active sites, including hemerythrin,¹⁹ ribonucleotide reductase,²⁰ methane monooxygenase,²¹ soybean lipoxygenase,²² and isopenicillin N synthase.²³

The six-coordinate complexes without nitrosyl ligands have areas ranging from 3.6 to 5.8 with one exception. The pre-edge peak area of $[\text{Fe}(\text{N-MeIm})_6](\text{BPh}_4)_2$ is the smallest, as expected, because this compound is the closest in symmetry to octahedral, with six nitrogen ligands at an average distance of 2.21 Å.²⁷ In fact, it was difficult to obtain a consistent value for its peak area, as the pre-edge feature was barely resolvable from the absorption edge. The next five complexes have mixed N/O coordination with five of the six ligands having similar bond distances and the sixth having one somewhat longer or shorter;^{28–32} this small distortion may account for the larger pre-edge intensities. The structures of $[\text{Fe}_2(\text{O}_2\text{CPh})_4(\text{pyridine})_4]$ and the cation of $[(6\text{TLA})\text{Fe}(\text{benzoylformate})](\text{ClO}_4)$ are shown

Table 1. Pre-Edge Data for Synthetic High-Spin Iron(II) Complexes

complex	first coordn sphere	$1s \rightarrow 3d^a$	ref
Six-Coordinate Complexes			
$[\text{Fe}(\text{N-Me-imidazole})_6](\text{BPh}_4)_2$	6 N	3.6	27
$[\text{Fe}_2(\text{O}_2\text{CPh})_4(\text{pyridine})_4]$	4 O, 2 N	3.7	28
$[\text{Fe}_2(\text{TPA})_2(\text{O}_2\text{CCH}_3)_2](\text{BPh}_4)_2$	4 N, 2 O	4.2	29
$[(6\text{TLA})\text{Fe}(\text{O}_2\text{CPh})](\text{ClO}_4)$	4 N, 2 O	4.3	30
$[\text{Fe}_2(\text{BPMP})(\text{O}_2\text{CCH}_3)_2](\text{BPh}_4)_2$	3 N, 3 O	4.4	31
$[(6\text{TLA})\text{Fe}(\text{benzoylformate})](\text{ClO}_4)$	4 N, 2 O	4.7	32
$[\text{Fe}_2(\text{TMPzA})_2\text{Cl}_2](\text{BPh}_4)_2$	4 N, 2 Cl	5.8	33
$[\text{Fe}(\text{cyclen})(\text{O}_2\text{CCH}_3)](\text{CF}_3\text{SO}_3)$	4 N, 1 O, 1 O (long)	9.7	28
Six-Coordinate Nitrosyl Complexes			
$[(\text{TMPzA})\text{Fe}(\text{NO})(\text{ClO}_4)](\text{ClO}_4)$	1 N _{NO} , 4 N, 1 O	9.4	34
$[(\text{TMPzA})\text{Fe}(\text{NO})(\text{Cl})](\text{BPh}_4)$	1 N _{NO} , 4 N, 1 Cl	11.4	23c
$[(\text{TPA})\text{Fe}(\text{BF})(\text{NO})](\text{ClO}_4)$	1 N _{NO} , 4 N, 1 O	12.8	35
Five-Coordinate Complexes			
$[(\text{HB}(3,5\text{-}^i\text{Pr}_2\text{pz})_3)\text{Fe}(\text{acac})]$	3 N, 2 O	7.8	36
$[\text{Fe}_2(\text{O}_2\text{CPh})_4(\text{pyridine})_2]$	4 O, 1 N	8.8	28
$[(\text{TPA})\text{Fe}(\text{SC}_6\text{H}_4\text{-}2,4,6\text{-Me}_3)](\text{ClO}_4)$	4 N, 1 S	8.9	23c, 37
$[\text{Fe}_2(\text{O}_2\text{C}(\text{CH}_3)_3)_4(\text{pyridine})_2]$	4 O, 1 N	9.0	28
$[(\text{HB}(3,5\text{-}^i\text{Pr}_2\text{pz})_3)\text{Fe}(\text{O}_2\text{CPh})]$	3 N, 2 O	10.7	38
$[\text{Fe}_2(\text{N-Et-HPTB})(\text{O}_2\text{CPh})](\text{BF}_4)_2$	3 N, 2 O	12.6	39
$[\text{Fe}_2(\text{HPTP})(\text{O}_2\text{CPh})](\text{BPh}_4)_2$	3 N, 2 O	13.4	39
Four-Coordinate Complexes			
$[(\text{HB}(3,5\text{-}^i\text{Pr}_2\text{pz})_3)\text{FeCl}]$	3 N, 1 Cl	16.4	40
$(\text{NEt}_4)_2[\text{FeCl}_4]$	4 Cl	17.4	26
$[(\text{HB}(3,5\text{-}^i\text{Pr}_2\text{pz})_3)\text{Fe}(\text{OC}_6\text{H}_4\text{-}p\text{-Cl})]$	3 N, 1 O	18.5	40
$[(\text{HB}(3,5\text{-}^i\text{Pr}_2\text{pz})_3)\text{Fe}(\text{SC}_6\text{H}_4\text{-}p\text{-NO}_2)]$	3 N, 1 S	21.0	40

^a Normalized area expressed in units of 10^{-2} eV.

in Figure 3. $[\text{Fe}_2(\text{TMPzA})_2\text{Cl}_2](\text{BPh}_4)_2$ has a even larger pre-edge area (5.8 units), most likely because of the two $\mu\text{-Cl}$ ligands that bridge the two iron centers asymmetrically ($\text{Fe}-\text{Cl} = 2.37, 2.58 \text{ \AA}$). Each iron center also has three $\text{Fe}-\text{N}$ bonds with an average length of 2.16 Å and one $\text{Fe}-\text{N}$ at 2.31 Å.³³ $[\text{Fe}(\text{cyclen})(\text{O}_2\text{CCH}_3)](\text{CF}_3\text{SO}_3)$ has a pre-edge area of 9.7 units that is even larger than those of some of the five-coordinate complexes surveyed. The large intensity may be a result of its asymmetrically chelated carboxylate ligand, which has $\text{Fe}-\text{O}$ bond distances of 2.04 and 2.35 Å.²⁸ The longer $\text{Fe}-\text{O}$ bond apparently is weak enough that the compound behaves more like a five-coordinate complex than a six-coordinate one.

The pre-edge peak areas of the nitrosyl complexes $[(\text{TMPzA})\text{Fe}(\text{NO})(\text{ClO}_4)](\text{ClO}_4)$, $[(\text{TMPzA})\text{Fe}(\text{NO})(\text{Cl})](\text{BPh}_4)$, and $[(\text{TPA})\text{Fe}(\text{BF})(\text{NO})](\text{ClO}_4)$ are unusually large for six-coordinate "iron(II)" complexes (9.4, 11.4, and 12.8, respectively). This is most probably due to significant distortion from octahedral symmetry caused by the short $\text{Fe}-\text{N}_{\text{nitrosyl}}$ bonds, which results in enhanced metal $3d-4p$ mixing. The crystal structures of the three complexes^{23c,34,35} all show a short $\text{Fe}-\text{N}$ bond of 1.70–1.77 Å with the remaining metal–ligand bonds ranging from 2.05 to 2.34 Å. The presence of short (1.74–1.80 Å) $\text{Fe}-\text{O}_{\text{oxo}}$ bonds in oxo-bridged diiron(III) complexes has also been found to give rise to significantly higher $1s \rightarrow 3d$ peak intensities (13 units) than are usually observed for hexacoordinate iron(III) complexes (6–9 units), for the same reason.⁵

The five-coordinate complexes have pre-edge peak areas ranging from 7.8 to 13.4 units. $[(\text{HB}(3,5\text{-}^i\text{Pr}_2\text{pz})_3)\text{Fe}(\text{acac})]$ has mixed oxygen and nitrogen coordination, but all five ligands

(27) Miller, L. L.; Jacobson, R. A.; Chen, Y.-S.; Kurtz, D. M., Jr. *Acta Crystallogr.* **1989**, *C45*, 527–529.

(28) Lachicotte, R. J.; Hagen, K. S. Unpublished results.

(29) Ménage, S.; Zang, Y.; Hendrich, M. P.; Que, L., Jr. *J. Am. Chem. Soc.* **1992**, *114*, 7786–7792.

(30) Zang, Y.; Elgren, T. E.; Dong, Y.; Que, L., Jr. *J. Am. Chem. Soc.* **1993**, *115*, 811–813.

(31) Borovik, A. S.; Hendrich, M. P.; Holman, T. R.; Munck, E.; Papaefthymiou, V.; Que, L., Jr. *J. Am. Chem. Soc.* **1990**, *112*, 6031–6038.

(32) Chiou, Y.-M.; Que, L., Jr. *J. Am. Chem. Soc.* **1992**, *114*, 7567–7568.

(33) Zang, Y.; Jang, H. G.; Chiou, Y.-M.; Hendrich, M. P.; Que, L., Jr. *Inorg. Chim. Acta* **1993**, *213*, 41–48.

(34) Zang, Y.; Ming, L.-J.; Que, L., Jr. Manuscript in preparation.

(35) Chiou, Y.-M. Ph.D. Thesis, University of Minnesota, 1994.

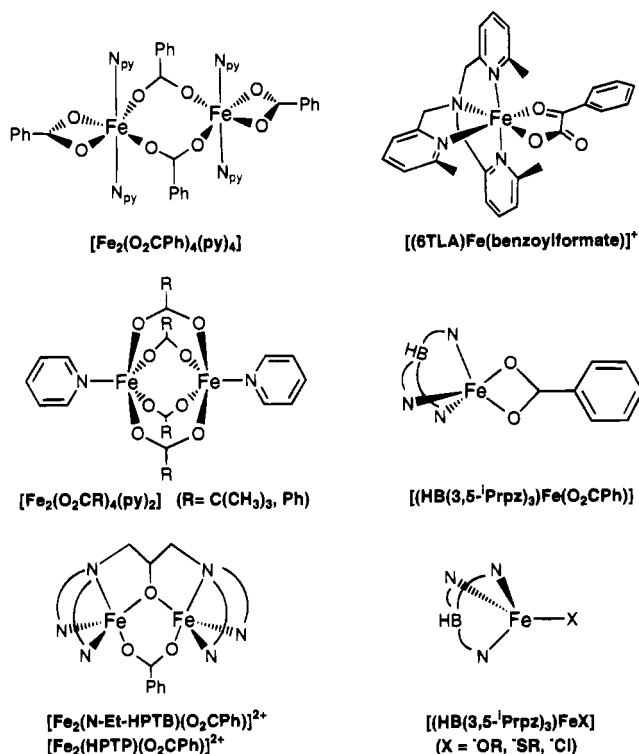


Figure 3. Structures of some of the iron(II) model complexes studied.

are at approximately the same distance from the iron center, consistent with its having the lowest pre-edge area among the five-coordinate complexes studied.³⁶ The next three complexes in ascending order of pre-edge area also have relatively high site symmetry at the iron center. Both $[\text{Fe}_2(\text{O}_2\text{CPh})_4(\text{pyridine})_2]$ and $[\text{Fe}_2(\text{O}_2\text{CC}(\text{CH}_3)_3)_4(\text{pyridine})_2]$ (Figure 3) have four bridging carboxylate ligands and one terminal pyridine ligand, affording approximate C_{4v} symmetry around each iron center.²⁸ $[(\text{TPA})\text{Fe}(\text{SC}_6\text{H}_2-2,4,6-\text{Me}_3)](\text{ClO}_4)$ ^{23c,37} has a tetradentate tripodal amine ligand and a thiolate ligand, giving it nearly C_{3v} symmetry at the iron atom. The remaining five-coordinate complexes are somewhat more distorted. The crystallographically characterized acetate analogue of $[(\text{HB}(3,5-\text{Pr}_2\text{pz})_3)\text{Fe}(\text{O}_2\text{CPh})]$ (Figure

3) has four N,O ligands at an average distance of 2.08 Å, with a more distant carboxylate oxygen atom at 2.23 Å.³⁸ Both $[\text{Fe}_2(\text{N-Et-HPTB})(\text{O}_2\text{CPh})](\text{BF}_4)_2$ and $[\text{Fe}_2(\text{HPTP})(\text{O}_2\text{CPh})](\text{BPh}_4)_2$ have dinucleating multidentate ligands, which provide each iron atom with three terminal amines, one bridging alkoxide, and a bridging carboxylate ligand (Figure 3).³⁹ Each iron center of $[\text{Fe}_2(\text{N-Et-HPTB})(\text{O}_2\text{CPh})](\text{BF}_4)_2$ has one Fe—O distance of ca. 1.97 Å, three similar Fe—N,O distances averaging 2.06 Å, and one Fe—N bond length of ca. 2.30 Å.³⁹

Only four four-coordinate iron(II) complexes were analyzed, as not many of these are known. These tetrahedral complexes^{26,40} exhibit pre-edge areas of 16.4–21.0 units, which are significantly larger than those of the five-coordinate complexes studied.

Thus, like the high-spin iron(III) complexes studied by Roe *et al.*, this series of high-spin iron(II) complexes exhibits a range of 1s → 3d pre-edge areas that can be used to deduce the coordination number and geometry of iron(II) complexes. Pre-edge spectra can be taken quickly as part of routine EXAFS data collection and readily analyzed. It is hoped that pre-edge studies will be used to complement EXAFS studies in order to gain further insight into the active-site coordination environments of the growing class of nonheme iron(II)-containing proteins. This technique has already been used successfully to determine the probable coordination geometries of isopenicillin N synthase and catechol 2,3-dioxygenase, their substrate complexes, and corresponding ES·NO adducts.^{23c,41}

Acknowledgment. This work was supported by the National Institutes of Health (Grant GM-33162). C.R.R. gratefully acknowledges a traineeship from the U.S. Public Health Service (Grant GM-07323).

Supplementary Material Available: Listings of X-ray crystallographic data, ORTEP plots, and tables of selected intramolecular bond lengths and angles for $[\text{Fe}_2(\text{O}_2\text{CPh})_4(\text{pyridine})_4]$, $[\text{Fe}(\text{cyclen})(\text{O}_2\text{CCH}_3)](\text{CF}_3\text{SO}_3)$, $[(\text{TMPzA})\text{Fe}(\text{NO})(\text{ClO}_4)](\text{ClO}_4)$, $[(\text{TMPzA})\text{Fe}(\text{NO})(\text{Cl})](\text{BPh}_4)$, $[\text{Fe}_2(\text{O}_2\text{CPh})_4(\text{pyridine})_2]$, and $[\text{Fe}_2(\text{O}_2\text{CC}(\text{CH}_3)_3)_4(\text{pyridine})_2]$ (19 pages). See any current masthead page for ordering information.

IC941243T

(36) Kitajima, N.; Amagai, H.; Tamura, N.; Ito, M.; Moro-oka, Y.; Heerwegh, K.; Pénicard, A.; Mathur, R.; Reed, C. A.; Boyd, P. D. *Inorg. Chem.* **1993**, *32*, 3583–3584.
 (37) Zang, Y.; Que, L., Jr. *Inorg. Chem.* **1995**, *34*, 1030–1035.

(38) Kitajima, N.; Fukui, H.; Moro-oka, Y.; Mizutani, Y.; Kitagawa, T. *J. Am. Chem. Soc.* **1990**, *112*, 6402–6403.
 (39) Dong, Y.; Ménage, S.; Brennan, B. A.; Elgren, T. E.; Jang, H. G.; Pearce, L. L.; Que, L., Jr. *J. Am. Chem. Soc.* **1993**, *115*, 1851–1859.
 (40) Ito, M. Ph.D. Thesis, Tokyo Institute of Technology, 1994.
 (41) Shu, L.; Chiou, Y.-M.; Orville, A. M.; Miller, M. A.; Lipscomb, J. D.; Que, L., Jr. *Biochemistry*, in press.